Optimizing Rainfall Estimates with the Aid of Radar

Edward A. Brandes

National Severe Storms Laboratory, NOAA, Norman, Okla. 73069

ABSTRACT

Estimates of precipitation are improved when raingage observations are used to calibrate quantitative radar data as well as to estimate precipitation in areas without radar data.

Estimated areal precipitation depth errors for nine rainfalls over a 3000 km² watershed averaged 13 and 14% (1.5 and 1.8 mm) when the radar was calibrated by networks of raingages having densities of one gage per 900 and 1600 km². Areal precipitation estimates derived from rainfalls observed at the gages alone produced errors of 21 and 24% (2.5 and 3.0 mm). Adjusting the radar data by a single calibration factor (the simple average ratio of gage-observed and radar-inferred rainfall at all input gages without regard to the spatial variation among ratios) resulted in error reduction to 18% (2.1 mm). Radar data added to gage observations also increased the explained variance in point rainfall estimates above that from gages alone, from 53 to 77% and 46 to 72% for the above gage densities.

1. Introduction

Hydrologic applications of radar data should increase with availability of processed digital radar data. Practical considerations of radar rainfall measurements, with a description of the National Severe Storms Laboratory (NSSL) WSR-57 data collection system, are given by Wilk and Kessler (1970). Radar-measured rainfall accuracy has been discussed by Joss *et al.* (1968), Woodley and Herndon (1970), Huff (1967) and Wilson (1970). Although radar measures precipitation areal variability accurately, absolute calibration against *in situ* measurements is highly desirable (Hitschfeld and Bordan, 1954).

Wilson (1970) has shown that radar-derived precipitation estimates, when calibrated with gage densities as low as one gage per 3400 km² (1000 n mi²), are more accurate than estimates from gages alone spaced one per 860 km² (250 n mi²). In Wilson's study, a single calibration factor (the sum of observed rainfalls at calibrating gages divided by the sum of the uncorrected radar estimates) was uniformly applied to the radar data. However, investigation by the author and others reveal large spatial variations in calibration factors. The present study shows that radar estimates can be improved by generating a calibration factor matrix that reflects these variations and aims to develop tools for combining radar and raingage observations under operational conditions to produce timely and accurate precipitation maps.

2. Outline of program logic

Radar and raingage data routines for producing areal and point precipitation estimates outlined in Fig. 1 briefly consist of the following steps. Radar reflectivities are converted to rainfall rates, and accumulated totals are transformed from polar to Cartesian coordinates. Raingage observations are then used to calibrate the radar data and generate precipitation estimates in areas where quantitative radar data are unavailable.

a. Uncalibrated radar precipitation field

To convert radar reflectivities into rainfall depths we begin with the Probert-Jones (1962) radar equation in the form

$$\overline{P_r} = \frac{\pi^3 C}{1024 \ln 2} P_t h G^2 \phi \theta \,|\,K\,|^2 Z_e / (\lambda^2 r^2), \qquad (1)$$

where the variables and characteristics of the NSSL radar system are given in Table 1 and the radar receiver has a logarithmic response.

After converting $\overline{P_r}$, the average power received in watts, to dBm (i.e., dB below 1 mW) and substituting the values listed in Table 1, we write (1) in the logarithmic form

$$\log Z_e = 0.1 \overline{P_r} + 7.73 + 2 \log r, \qquad (2)$$

where r is the radar slant range (km). The second term on the right-hand side includes a correction for the difference between $\overline{\log P_r}$ and $\log \overline{P_r}$ (2.5 dB) and an assumed 2.0 dB radome two-way attenuation (Curtis and Vaccaro, 1961). Additional adjustments to $\overline{P_r}$ are made for atmospheric absorption (Blake, 1970), rainfall attenuation (Burrows and Attwood, 1949), and
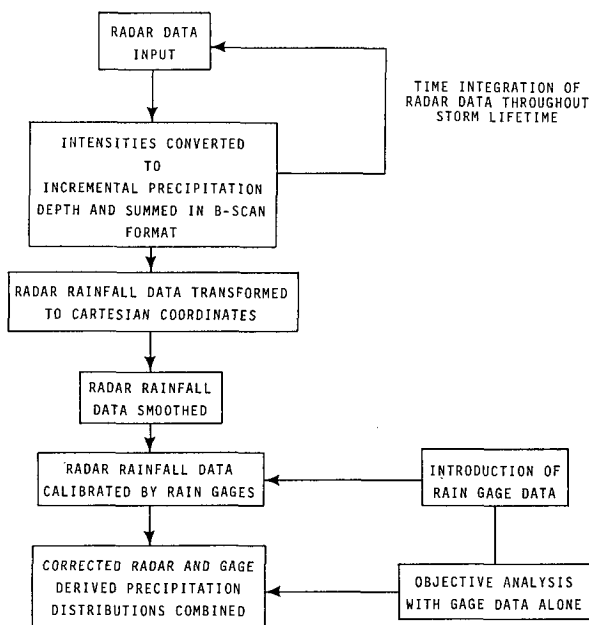
Fig. 1. Analysis scheme.

During 1974, precipitation echoes from the NSSL WSR-57 radar were quantized into 64 intensity classes having a width of 1.2 dB. Spatial resolution was dictated by the antenna beam width (2°), range averaging interval (1 km), equivalent averaging time (0.19 s), antenna angular velocity (18° s⁻¹), and azimuthal recording interval (2°) (Sirmans and Doviak, 1973). Rainfall rates calculated for each data point are multiplied by the time between observations, usually 5 min in the test data, to obtain incremental precipitation depths. Rainfalls are summed in B-scan (azimuth-range) format and converted to rectilinear display. Only data taken at zero antenna elevation are considered in this study. Analysis grid elements are assigned the accumulated depth of the particular data gate in which the grid points reside. The analysis grid spacing of 2.32 km (1.25 n mi) corresponds closely with the radar resolution and only small errors are introduced by this scan conversion.

The rainfall field derived from radar data alone is lightly filtered to reduce small-scale fluctuations. Smoothed grid values of radar rainfall, $A_s(I, J)$, are determined from a nine-point operator (Shuman, 1957):

$$A_s(I,J) = A(I,J) + \frac{a}{2}(1-a)[A(I, J+1) + A(I, J-1)$$

$$+ A(I+1, J) + A(I-1, J) - 4A(I,J)]$$

$$+ \frac{a^2}{4}[A(I+1, J+1) + A(I+1, J-1)$$

$$+ A(I-1, J+1) + A(I-1, J-1) - 4A(I,J)],$$

$$(4)$$

with $a = \frac{1}{2}$. With this operator wavelengths of four grid lengths are smoothed to 50% of their original amplitude, while wavelengths longer than 12 grid lengths are essentially unchanged.

for reflectivity estimate bias in regions of high rainfall gradient (Rogers, 1971; Sirmans and Doviak, 1973). Corrections for standard atmosphere absorption vary from approximately 0.8 dB at 40 km to 1.4 dB at 80 km. Rainfall attenuation is generally less than 1 dB except for long radar penetration paths through high rainfall rates. Although gradient bias errors for a single radar measurement can be very large (>10 dB), for a watershed this error is usually less than 1 dB even for highly convective rainfalls.

Rainfall rates (R, mm h⁻¹) are estimated with the familiar Z-R expression

$$Z_e = 200R^{1.6}. \qquad (3)$$

The described methodology minimizes the impact of the Z-R relationship and the need for an absolute radar calibration because the raingage values are used to adjust the radar measurements.

b. Calibrated radar field

The smoothed radar field is then calibrated with raingage observations by determining multiplicative calibration factors at each raingage site recording at least 2.5 mm (0.10 inch) precipitation. Gages recording less than 2.5 mm are not used because small differences between observed amounts and uncalibrated radar data can lead to spuriously large or small calibration factors. Averaged accumulated raw radar data from gates (2°×1 km) whose centers fall within 3.0 km of the gage site are divided into the gage amount to determine calibration factors.

Barnes' (1964) objective analysis scheme is used to move correction factors from raingage sites onto the grid point field. The weight (WT_i) each gage

TABLE 1. Definitions of radar equation terms and characteristics of the 1974 NSSL WSR-57 radar system.

$\bar{P}_r$	Average power received (W)	
P_t	Peak transmitted power (W)	2.26×10⁵
h	Pulse length (m)	1260
G^2	Antenna gain squared	4.169×10⁷
ϕ	Vertical beam width (deg)	2
θ	Horizontal beam width (deg)	2
$\lvert K \rvert^2$	Dielectric factor	0.93
Z_e	Equivalent reflectivity factor (mm⁶ m⁻³)	
r	Slant range (km)	
λ	Wavelength (cm)	10.6
C	Units conversion (rad² cm² m² km² deg⁻² mm⁻⁶)	3.046×10⁻²⁴

calibration (G_i) receives at a particular grid point is

$$WT_i = \exp(-d^2/EP),\qquad(5)$$

where d is the distance (km) between the gage and grid point. EP controls the degree of smoothing and is kept as small as possible to preserve detail in the input observations. For example, when $EP = 600$ km² about 25% of the amplitude of a 60 km wavelength is retained; this value increases to 60% when EP $= 200$ km². Fig. 2 presents the relationship between observation weight and distance for several values of EP. Specific values are determined by input data spacing, wavelengths of interest, and estimated observational error. Weighting constants utilized in the analysis are given in Table 2. At distances roughly equivalent to the mean station spacing, weights given calibration factors varied from 0.03 to 0.05. Observations are ignored when their weight is less than a prescribed value (ME).

Selection of ME and EP essentially define an observation's maximum region of influence. To insure consideration of more than one gage-radar comparison at each grid point, an influence radius of 70 km was selected for individual calibration factors. At grid locations more than 70 km from a calibration site the average of all gage factors is used.

Two passes through the objective analysis grid are made with the input data to produce the radar calibration field. On the first pass, a first-guess grid point calibration (F_1) is computed as

$$F_1 = \sum_{i=1}^{N} WT_i G_i / \sum_{i=1}^{N} WT_i,\qquad(6)$$

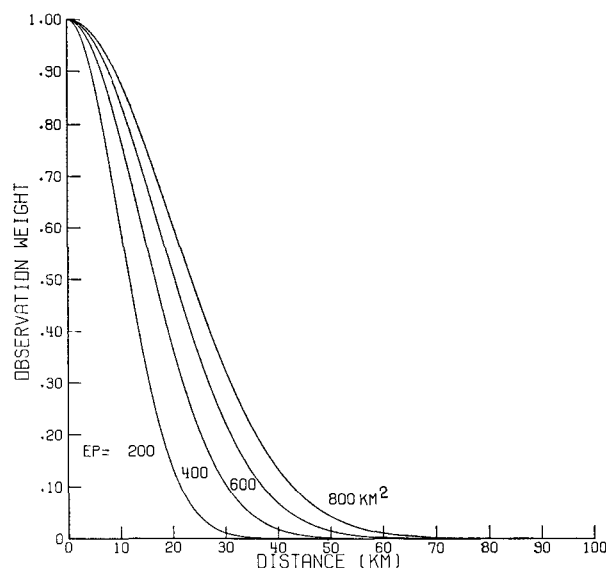where N is the number of gages.

FIG. 2. Gage observation weight as a function of distance for various weighting factors (EP).

TABLE 2. Initial objective analysis weighting constants (EP)

	Input gage density	
	1 gage per 900 km²	1 gage per 1600 km²
Radar calibration field	300 km²	450 km²
Gage-derived precipitation field	200 km²	350 km²

Differences (D_i) are calculated at each gage location from

$$D_i = G_i - F_1,\qquad(7)$$

where the first-guess estimate (F_1) is taken at the grid point nearest the raingage rather than at the gage itself.[1]

The second pass uses (5) with EP reduced by 50% and analyzes the differences (errors) at each observation site by the same method. Difference values (corrections) calculated at each grid point are added to the first-guess field and the final grid point calibration, generally determined from calibration data of more than one calibrating gage, is given by

$$F_2 = F_1 + \sum_{i=1}^{N} WT_i D_i / \sum_{i=1}^{N} WT_i.\qquad(8)$$

Multiplication of the calibration field with the lightly smoothed radar field produces the corrected (calibrated) radar precipitation field. In reality, the radar precipitation field has been molded to fit gage observations while retaining radar-observed precipitation variation between gages. Further discussion of the objective analysis technique can be found in Barnes (1973).

c. Gage-derived precipitation field

All available raingage data, including previously omitted gages recording less than 2.5 mm and gages in regions without quantitative radar data, are used for a second objective analysis of the precipitation field. In areas without quality radar data, this is the only precipitation estimate. The procedure is similar to that already outlined.[2] A smaller EP value is used (Table 2) to preserve detail contributed by the additional gage observations. At the mean station spacing distance, rainfall observations had a weight of approximately 0.01. Maximum radius of influence for this estimate is defined as the distance at which storm total rainfalls become essentially uncorrelated. For Oklahoma convective rainfalls this distance is approximately 90 km (Fig. 3).

---

[1] This approximation introduces negligible error since in our study the maximum distance from a raingage to the nearest grid point never exceeds 1.2 km. For applications with larger grid spacings, F_1 (at the gage site) could be bilinearly interpolated to the gage from surrounding grid points.

[2] An application of the Cressman (1959) analysis method to raingage data is described by Maine and Gauntlett (1968).
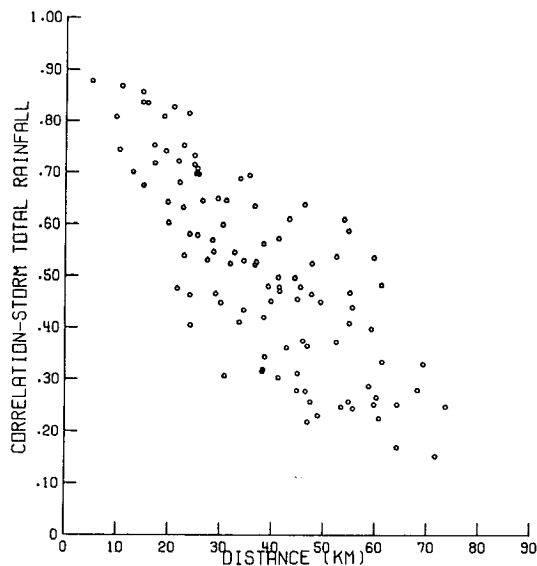
FIG. 3. Correlation between storm rainfall totals measured by raingages.

FIG. 5. Final precipitation analysis for 28–29 April 1974. Plotted values are calibration factors.

The gage-derived field is more exact at gage sites than the corrected radar field because the weighting factor EP has been reduced and calibration factors for the gage-calibrated radar data were averaged about the gage sites. Although gage-derived fields can be made to fit the input data exactly, it is desirable to allow some smoothing as compensation for errors inherent in raingage observations. Input gage observations and estimates interpolated to gage sites from either calibrated radar fields or gage-derived fields usually differed by 1 mm or less.
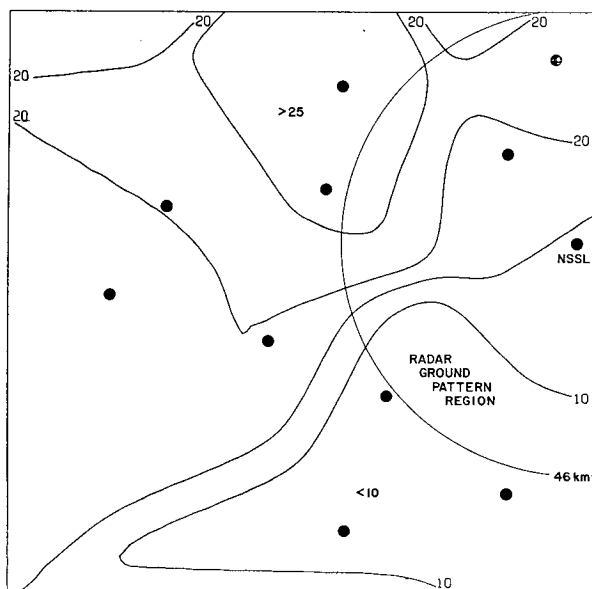

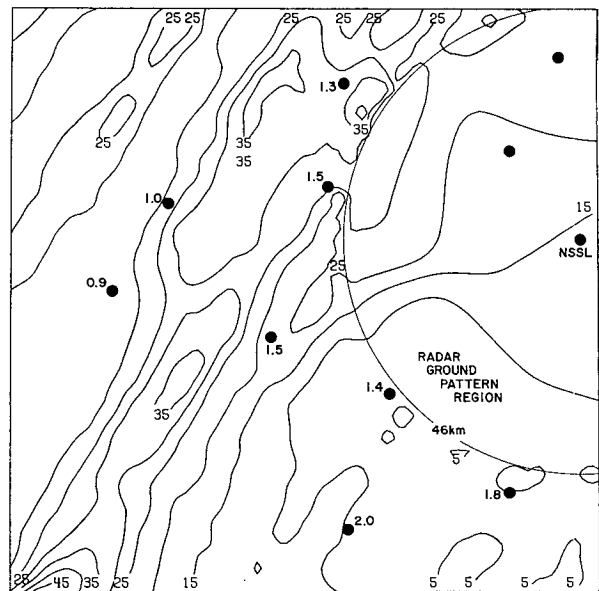FIG. 4. Gage-derived precipitation field for 28–29 April 1974, Depths are in millimeters.

d. Combined precipitation field

Corrected radar and gage-estimated rainfall distributions are combined with emphasis placed on the calibrated radar field. In the radar ground clutter region, at excessive distances from the radar, when radar data are incomplete (e.g., due to power failures), or where anomalous propagation has obscured precipitation echoes, only the precipitation field derived from gage observations is used. Where only one source indicates precipitation, it is considered to indicate true precipitation.

An example of a computer-contoured gage-derived field is shown in Fig. 4 and the combined precipitation field in Fig. 5. The combined precipitation field illustrates that precipitation gradients may be introduced at boundaries separating fields derived exclusively either from calibrated radar or raingage data (e.g., the radar ground pattern edge). Raingage-derived fields typically indicate larger characteristic lengths than are contained in the actual precipitation and radar fields. This is because of the wide spacing between gages relative to the precipitation scale. Evaporation below the radar beam, wind velocity fluctuations, and sampling are thought to be major contributors to large spatial variations among calibration factors (Fig. 5).

3. Application and evaluation

Nine convective precipitation events lasting from 2 to 11 h were selected for this study. The analysis area was approximately 170 km×170 km with a grid spacing of 2.32 km (1.25 n mi). Radar data within the analysis region were calibrated with factor fields

determined from two raingage networks and with the arithmetic average of all available calibration factors. Average estimated precipitation depths were computed for the Washita watershed, a 4000 km² subsection of the analysis grid located just west of NSSL. Gage densities in the primary analysis region (approximately one gage per 900 and 1600 km², i.e., 14 and 9 gages; Fig. 6) correspond roughly to that of the climatological raingage network. Approximately 25% of the watershed area is within the radar ground pattern but attention is focused on that region outside the radar ground clutter so that direct comparison can be made between calibrated radar- and gage-derived precipitation fields. Actual average depths of rainfall in the smaller watershed were calculated from 118 uniformly spaced raingages operated by the Agriculture Research Service (ARS), U. S. Department of Agriculture. Two aspects of the technique—how well the average watershed precipitation was estimated and how well the spatial variance within the watershed was described—are now considered.

Individual storm statistics at key steps in the analysis and average watershed precipitation depth errors are given in Tables 3 and 4. Large errors in the raw radar estimates, probably meteorological in origin, are typical (see, e.g., Woodley and Herndon, 1970) and illustrate the need for calibration. When raw radar estimates were multiplied by the simple average of all available calibration factors, without

TABLE 3. Estimated rainfalls (mm) for nine storms.

| | | Gage network density | | | | | |
| | | 1 gage per 900 km² | | 1 gage per 1600 km² | | Actual (ARS gages) | Average calibration factor* |
Storm	Raw radar	Gages alone	Cali-brated radar	Gages alone	Cali-brated radar		
1	15.5	17.5	19.7	18.2	19.8	21.0	1.54
2	7.6	13.7	15.0	11.1	13.5	17.4	2.33
3	8.7	26.4	27.6	29.6	27.4	28.7	2.99
4	16.8	10.0	14.5	9.7	13.7	10.4	0.71
5	8.5	4.8	5.4	4.4	5.5	5.2	0.54
6	9.7	12.6	9.6	11.5	11.6	8.7	1.23
7	18.8	25.5	21.4	22.5	22.3	22.4	1.07
8	14.6	6.2	9.8	5.9	8.2	9.8	0.76
9	18.1	6.4	6.7	4.8	7.8	9.2	0.68

* Simple average of calibration factors computed at all gages recording 2.5 mm or more.

regard for spatial variation among factors, estimate errors were 18% or 2.1 mm. Average errors in depth estimates made with radar data calibrated by the two gage networks were 13 and 14% (1.5 and 1.8 mm) and errors with gage observations alone were 21 and 24% (2.5 and 3.0 mm). Further testing will be required to determine the role of radar sampling frequency in the above results and to more fully develop the relationship between calibration gage distribution and estimate error.

Fig. 7 shows that the relative dispersions of precipitation (standard deviation times 100% divided by the mean) in the calibrated radar analysis agree closely but are slightly less than actual dispersions calculated from the dense ARS gage network. Huff (1967) has noted that dense gage data usually have larger dispersions than those observed by radar. The filtering operation described in Section 2 reduced dispersion in the uncalibrated radar data by approximately 3%. While the calibrated radar field preserves most of the areal precipitation variation, analyses with small numbers of input gage observations obviously results in substantial smoothing.

Statistics of point precipitation estimates computed from both calibrated radar and gage-derived precipita-
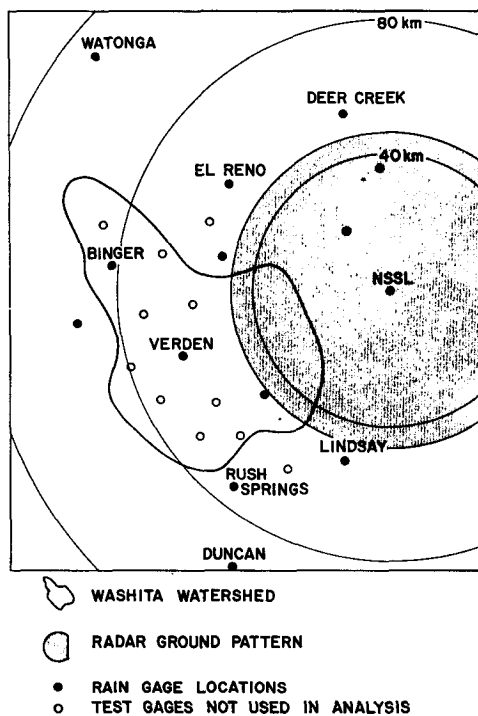

FIG. 6. Primary analysis region showing gage and watershed locations. Densities of unlabeled and labeled gages are approximately 1 gage per 900 and 1600 km².

TABLE 4. Comparison of estimated and actual average watershed depth (9 cases).

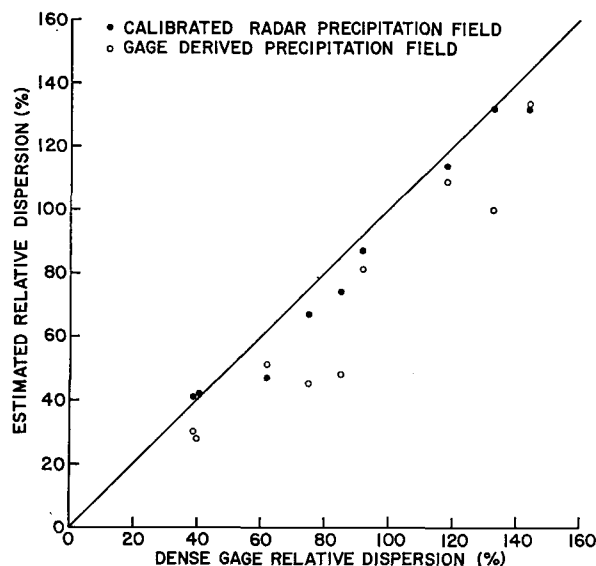| | Average estimate error | |
	(%)	(mm)
Raw radar	52	7.1
Radar calibrated by average factor	18	2.1
Radar calibrated by gage networks		
1 gage per 900 m²	13	1.5
1 gage per 1600 km²	14	1.8
Input gage depth		
1 gage per 900 km²	21	2.5
1 gage per 1600 km²	24	3.0

FIG. 7. Scattergram of relative dispersion in calibrated radar and gage-derived fields compared to precipitation dispersion determined from 118 ARS raingages. Density is 900 km² per gage.
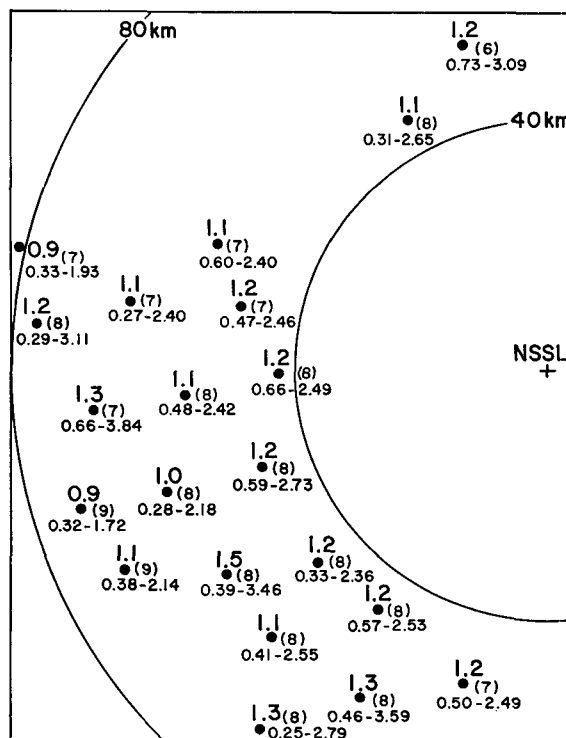

FIG. 8. Average calibration (gage to radar ratio) field for the NSSL mesonetwork (10 storms). Plotted data include the number of rainfall events ≥2.5 mm (in parentheses) and the range of calculated factors. The average storm calibration has been substituted whenever gage rainfalls were <2.5 mm.

tion fields for several test locations interspaced among the calibration gages (see Fig. 6) are compared in Table 5. Improved correlation with corrected radar data is expected since the calibrated radar field is molded to fit the gage observations and the radar-observed precipitation variance between gages is retained. The added value of radar in this sample is indicated by increased explained variance in depth estimates above that found by gages alone from 53 to 77% and from 46 to 72% for the two gage network densities.

Errors in calibrated radar and raingage fields differ in origin. Widely spaced gage data are subject to errors because distances between gages are larger than the precipitation element scale. Calibrated radar error results from small-scale variations that remain in the radar precipitation field between gages after calibration using widely spaced gages. Changes in the Z-R relationship, beam filling problems, and propagation anomalies probably contribute to these small-scale

TABLE 5. Correlation coefficient and explained variance between estimated and observed rainfall depths at test gages not used for calibration (95 events).*

	Gage density			
	1 gage per 900 km²		1 gage per 1600 km²	
	ρ	$\sigma_E{}^2$	ρ	$\sigma_E{}^2$
Calibrated radar estimate	0.88	77	0.85	72
Estimate from input gage amounts	0.73	53	0.68	46

* $\sigma_E{}^2$, explained variance (percent); ρ, correlation between estimated and observed rainfall depths.

variations. A plot of average calibration factors determined at NSSL mesonetwork sites for 10 rainfall events given in Fig. 8 reveals large spatial differences. It may be that ground targets distant from the radar are enhanced by ducting while it rains (note the small-scale rainfall maxima at the edge of ground pattern in Fig. 5). Battan (1959) described a condition of "thunderstorm super-refraction" in which local temperature inversions and specific humidity variations can produce strong ducting near thunderstorms. Since all storms examined were convective in character and may have had common properties, similarities in radar signal propagation are likely. Also, fixed ground targets close to the radar (e.g., trees, buildings, hills) may block or distort the radar beam causing systematic reflectivity errors.

4. Summary

A logical procedure has been developed for combining radar data with raingage observations to improve precipitation estimates. Gage observations are used to derive a field of radar calibration factors and to provide precipitation estimates in areas without quality radar data (e.g., in ground clutter regions, at excessive distances from the radar, and in areas

where there is anomalous propagation). For a small number of test cases, a radar-raingage combination significantly reduced the average error in areal precipitation estimated from gages alone for gage densities corresponding to the climatic network station spacing. The addition of radar data also increased the explained variance of point rainfall estimates.

Spatial fluctuations in average gage to radar ratio fields suggest that propagation effects, including local radar beam blocking, may cause recurring precipitation estimate errors.

REFERENCES

Barnes, S. L., 1964: A technique for maximizing details in numerical weather map analysis. *J. Appl. Meteor.*, **3**, 396–409.
——, 1973: Mesoscale objective map analysis using weighted time-series observations. NOAA Tech. Memo. ERL NSSL-62, Norman, Okla. 60 pp. [Available NTIS, No. COM-73-10781.]
Battan, L. J., 1959: *Radar Meteorology*. The University of Chicago Press, 161 pp.
Blake, L. V., 1970: Prediction of radar range. *Radar Handbook*, M. I. Skolnik, Ed., McGraw-Hill, 2-51 to 2-55.
Burrows, C. R., and S. S. Attwood, 1949: *Radio Wave Propagation*. Consolidated Summary Technical Report, Committee on Propagation, NDRC, Academic Press, p. 219.
Cressman, G. P., 1959: An operational objective analysis system. *Mon. Wea. Rev.*, **87**, 367–374.
Curtis, R. B., and J. Vaccaro, 1961: Survey of ground radomes. Report No. RAOC-TR-61-52, Rome Air Development Center, Griffiss AFB, N. Y.
Hitschfeld, W., and J. Bordan, 1954: Errors inherent in the radar measurement of rainfall at attenuating wavelengths. *J. Meteor.*, **2**, 58–67.
Huff, F. A., 1967: The adjustment of radar estimates of storm mean rainfall with raingage data. *J. Appl. Meteor.*, **6**, 52–56.
Joss, J., J. C. Thams and A. Waldvogel, 1968: The accuracy of daily rainfall measurements by radar. *Preprints 13th Conf. Radar Meteorology*, Montreal, Canada, Amer. Meteor. Soc., 448–451.
Maine, R., and D. J. Gauntlett, 1968: Modifications to an operational numerical weather analysis system and application to rainfall. *J. Appl. Meteor.*, **7**, 18–28.
Probert-Jones, J. R., 1962: The radar equation in meteorology. *Quart. J. Roy. Meteor. Soc.*, **88**, 485–495.
Rogers, R. R., 1971: The effect of variable target reflectivity on weather radar measurements. *Quart. J. Roy. Meteor. Soc.*, **97**, 154–167.
Shuman, F. G., 1957: Numerical methods in weather prediction: II. Smoothing and filtering. *Mon. Wea. Rev.*, **85**, 357–361.
Sirmans, D., and R. J. Doviak, 1973: Meteorological radar signal intensity estimation. NOAA Tech. Memo. ERL-NSSL-64, Norman, Okla. 80 pp. [Available from NTIS, No. COM-73-11923/2AS.]
Wilk, K. E., and E. Kessler, 1970: Quantitative radar measurements of precipitation. *Meteor. Mono.*, **11**, No. 33, 315–329.
Wilson, J. W., 1970: Integration of radar and raingage data for improved rainfall measurement. *J. Appl. Meteor.*, **9**, 489–497.
Woodley, W., and A. Herndon, 1970: A raingage evaluation of the Miami reflectivity-rainfall rate relation. *J. Appl. Meteor.*, **9**, 258–263.